The Cryosphere

Open Access

EGU
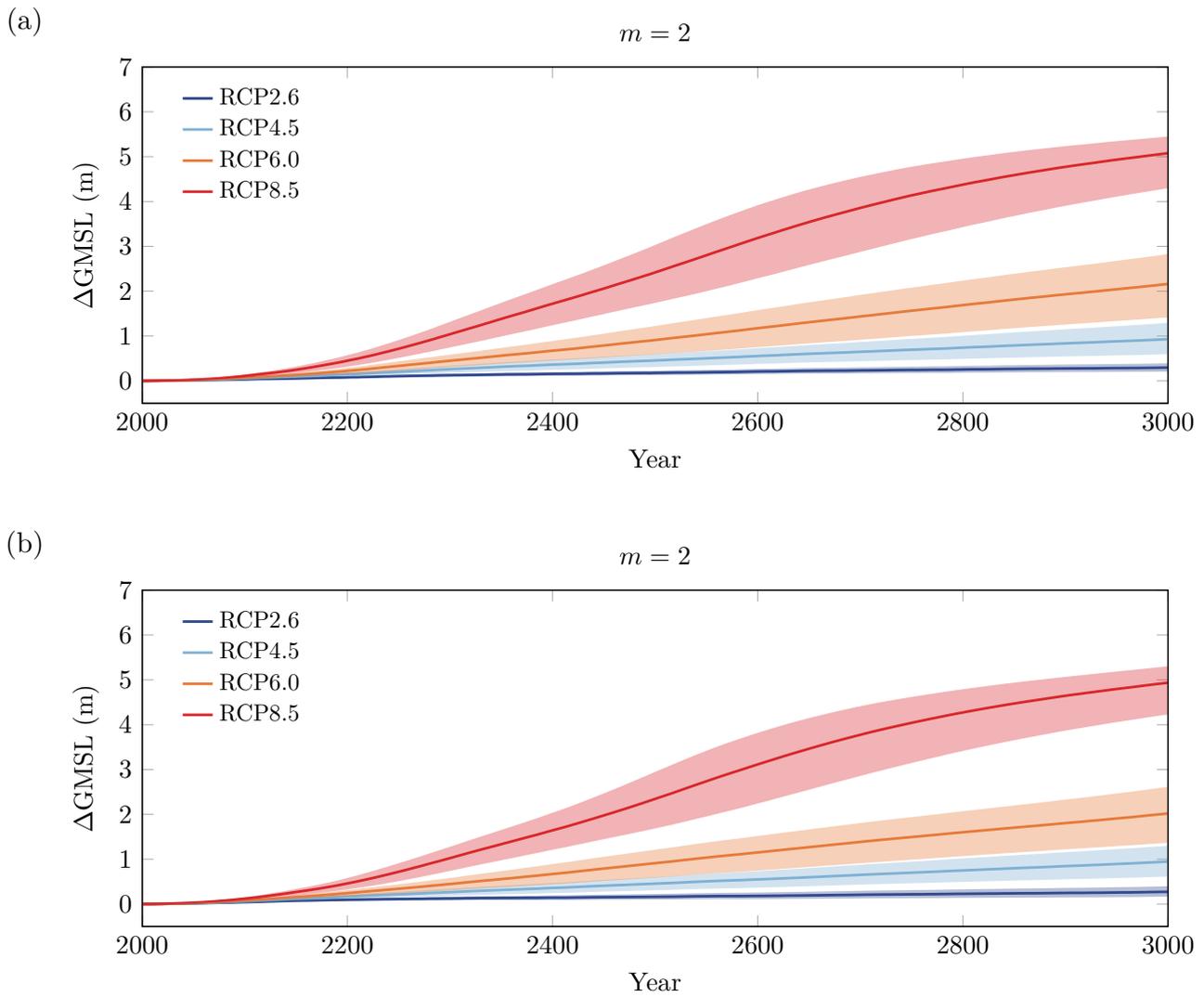
Supplement of

Uncertainty quantification of the multi-centennial response of the Antarctic ice sheet to climate change

Kevin Bulthuis et al.

*Correspondence to:* Kevin Bulthuis (kevin.bulthuis@uliege.be)

**Figure 1.** Comparison of Antarctic ice-sheet contribution to sea level under Weertman's sliding law with exponent $m = 2$ as a function of spatial resolution (20 km vs 16 km). (**a**) Spatial resolution of 20 km and (**b**) spatial resolution of 16 km. Solid lines are the median projections and the shaded areas are the 33–66 % probability intervals that represent the parametric uncertainty in the model.

1
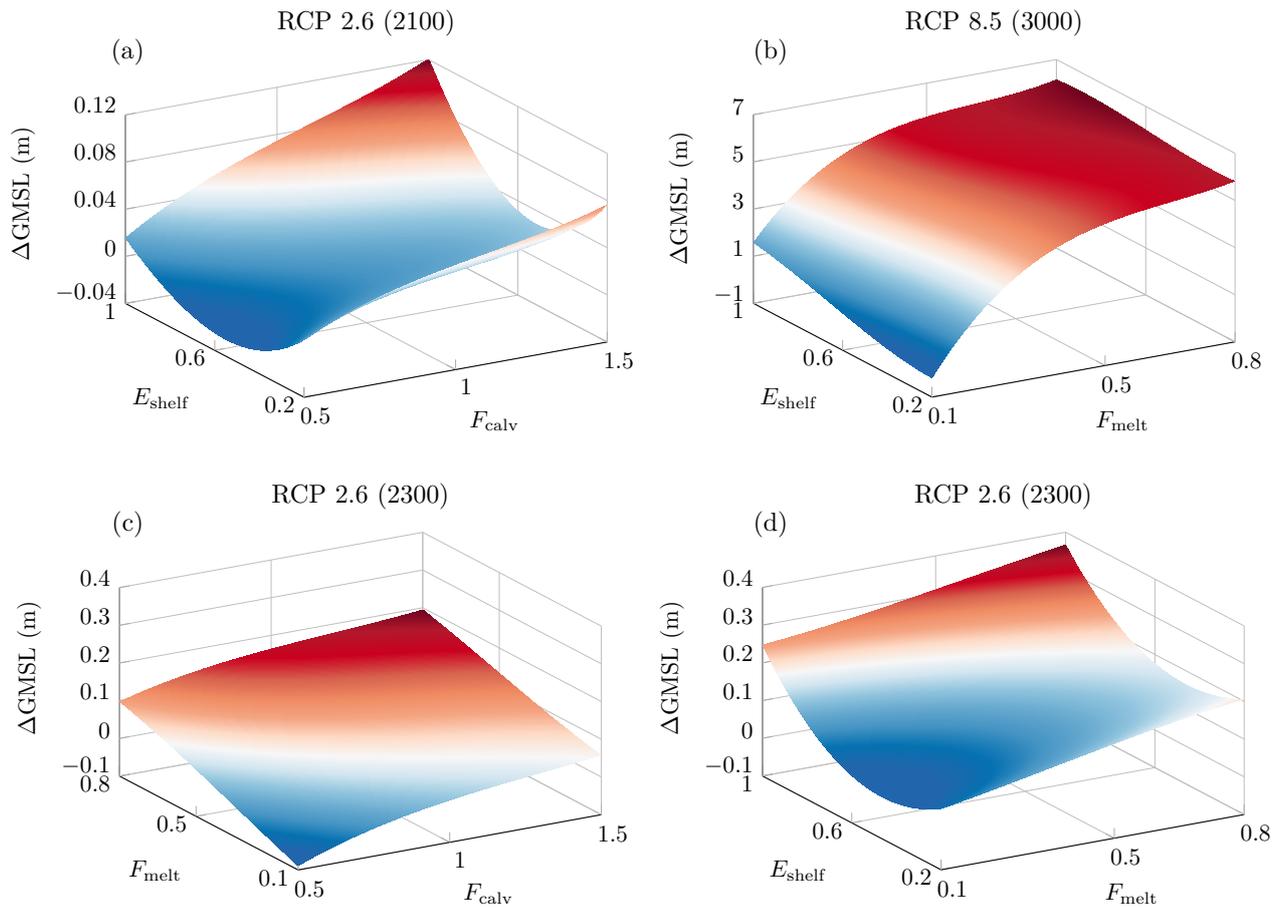
Figure 2. Representation of the emulators for pairs of parameters with other parameters fixed at their nominal value. Results are under Weertman's sliding law with exponent $m = 2$. Emulators (**a**) at 2100 in RCP 2.6 for the pair $(F_{\text{calv}}, E_{\text{shelf}})$, (**b**) at 2300 in RCP 8.5 for the pair $(F_{\text{melt}}, E_{\text{shelf}})$, (**c**) at 2300 in RCP 2.6 for the pair $(F_{\text{calv}}, F_{\text{melt}})$ and (**d**) at 3000 in RCP 2.6 for the pair $(F_{\text{melt}}, E_{\text{shelf}})$.
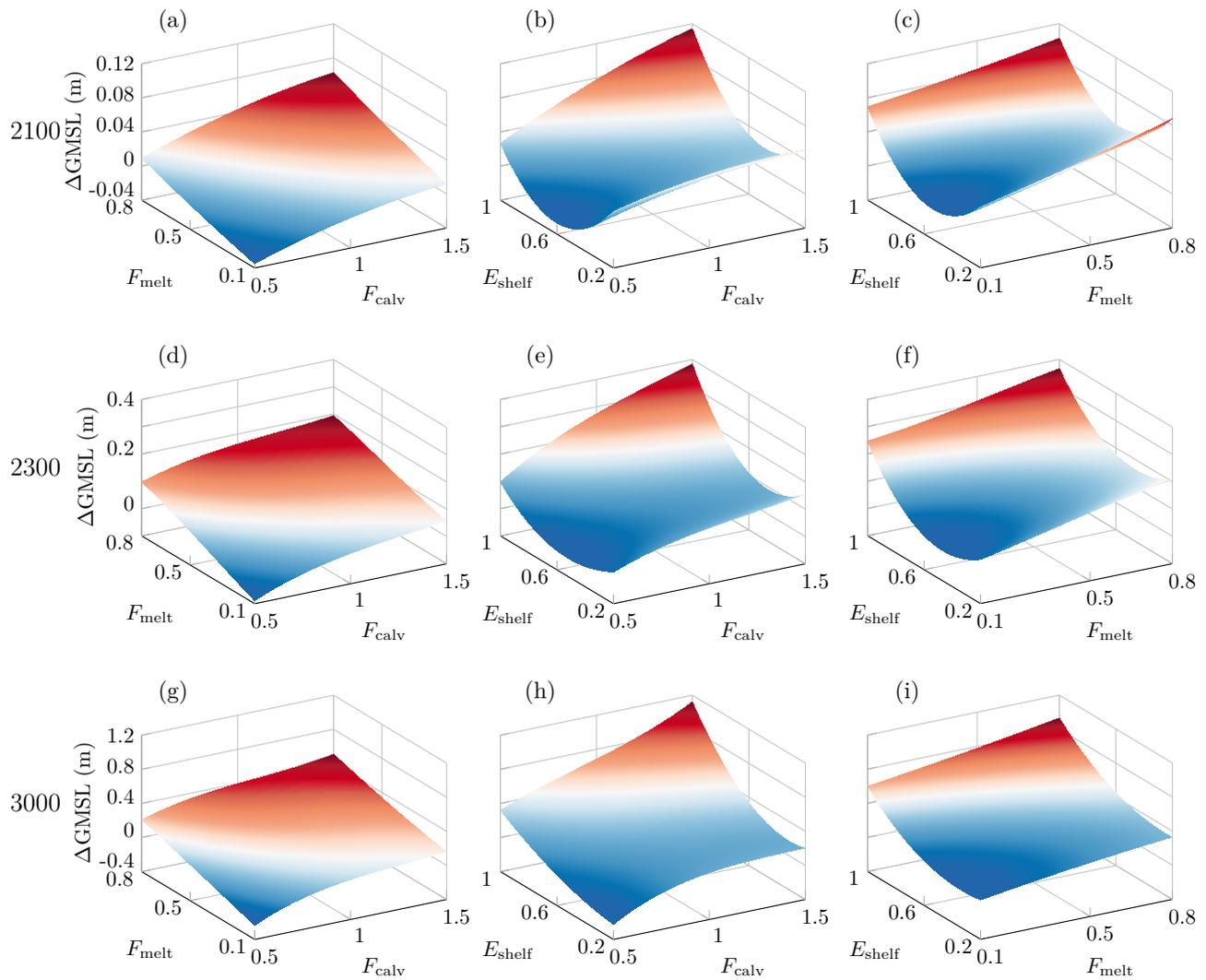
Figure 3. Representation of the emulators for pairs of parameters with other parameters fixed at their nominal value. Results are for the RCP 2.6 scenario under Weertman's sliding law with exponent $m = 2$. Emulators at 2100 (**a**, **b**, **c**), emulators at 2300 (**d**, **e**, **f**) and emulators at 3000 (**f**, **g**, **i**).
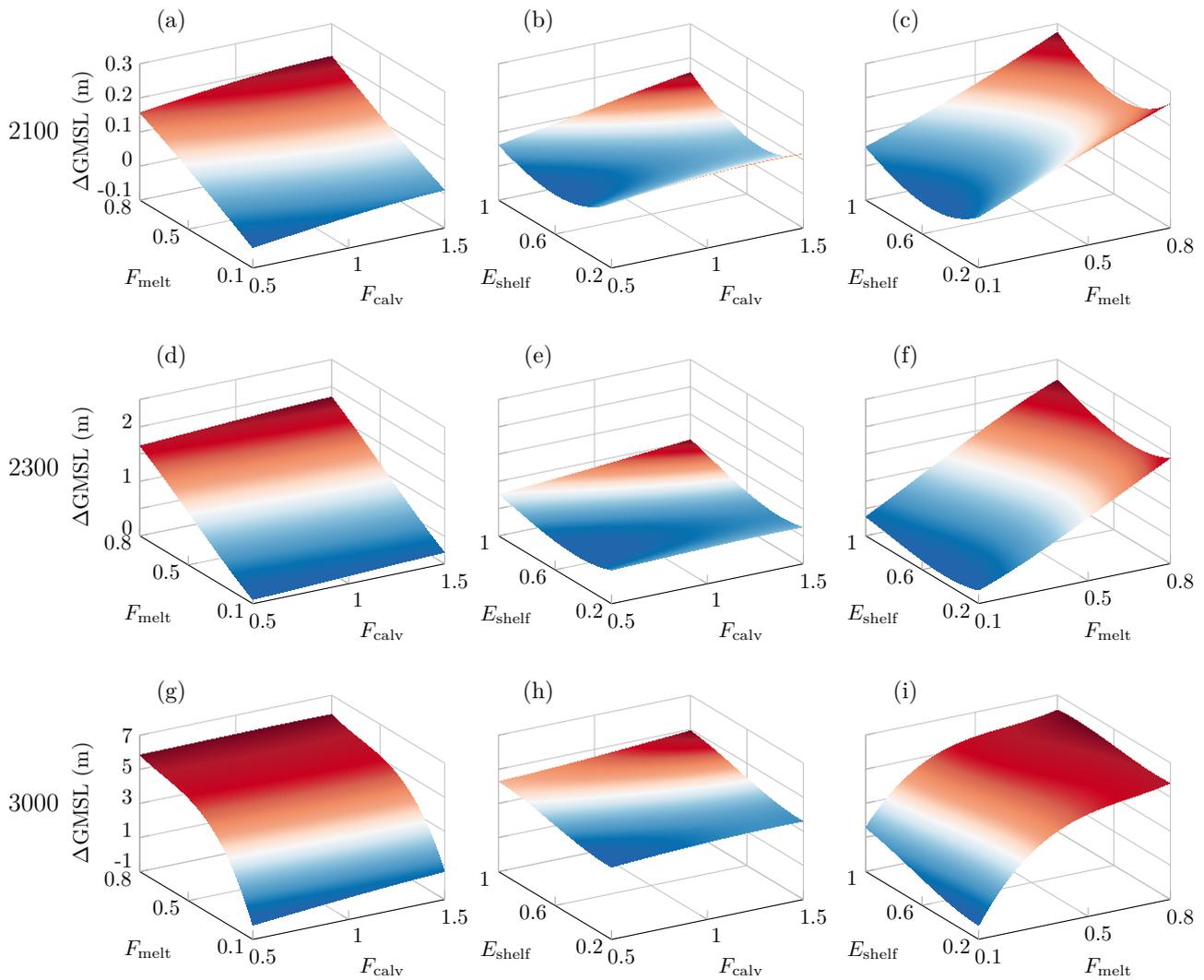
Figure 4. Representation of the emulators for pairs of parameters with other parameters fixed at their nominal value. Results are for the RCP 8.5 scenario under Weertman's sliding law with exponent $m = 2$. Emulators at 2100 (**a**, **b**, **c**), emulators at 2300 (**d**, **e**, **f**) and emulators at 3000 (**f**, **g**, **i**).
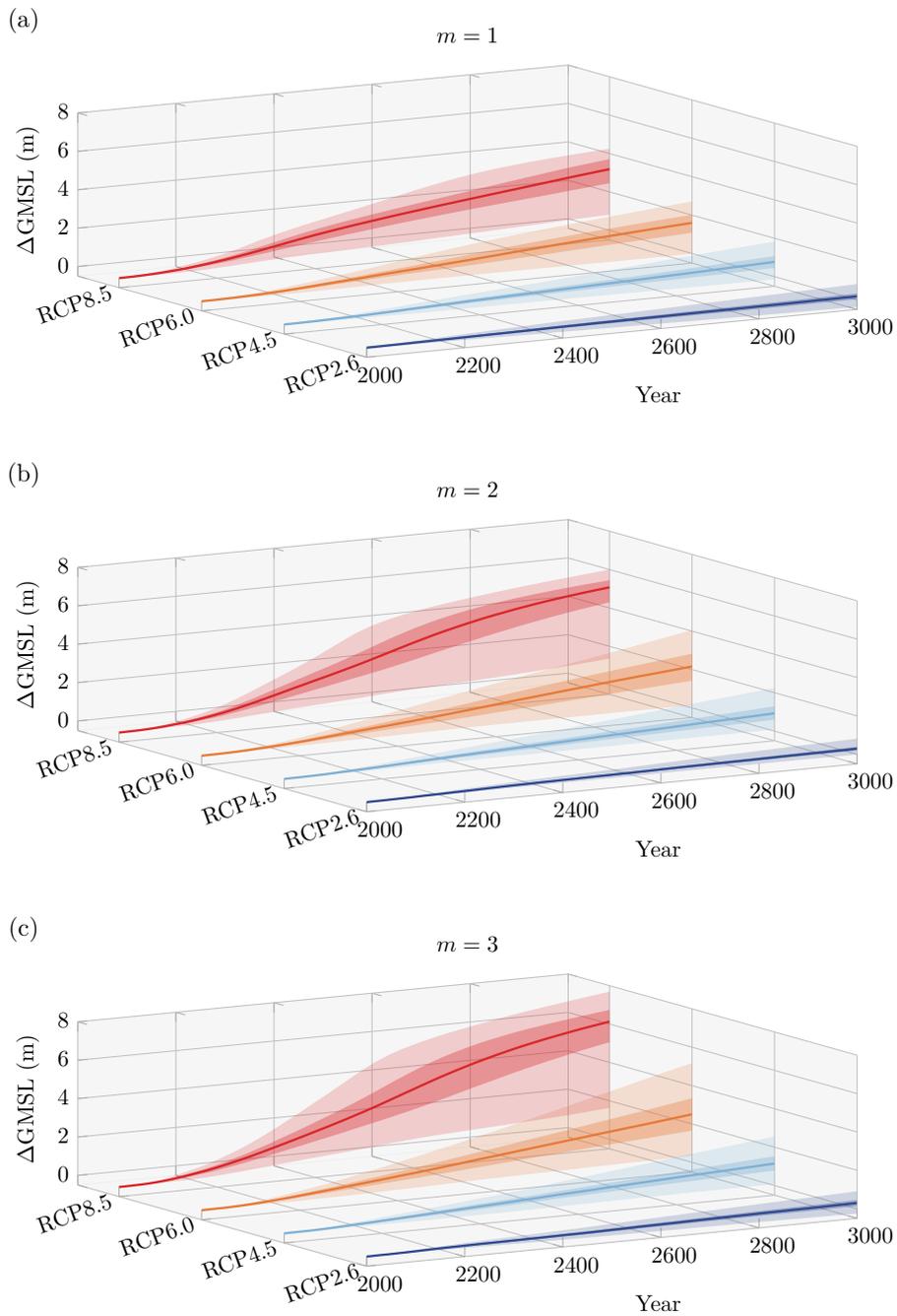
Figure 5. Antarctic ice-sheet contribution to global mean sea level relative to 2000. (**a**) Viscous sliding law, (**b**) weakly nonlinear sliding law and (**c**) strongly nonlinear sliding law. Solid lines are the median projections, the darker and lighter shaded areas are respectively the 33–66 % and 5-95 % probability intervals that represent the parametric uncertainty in the model.
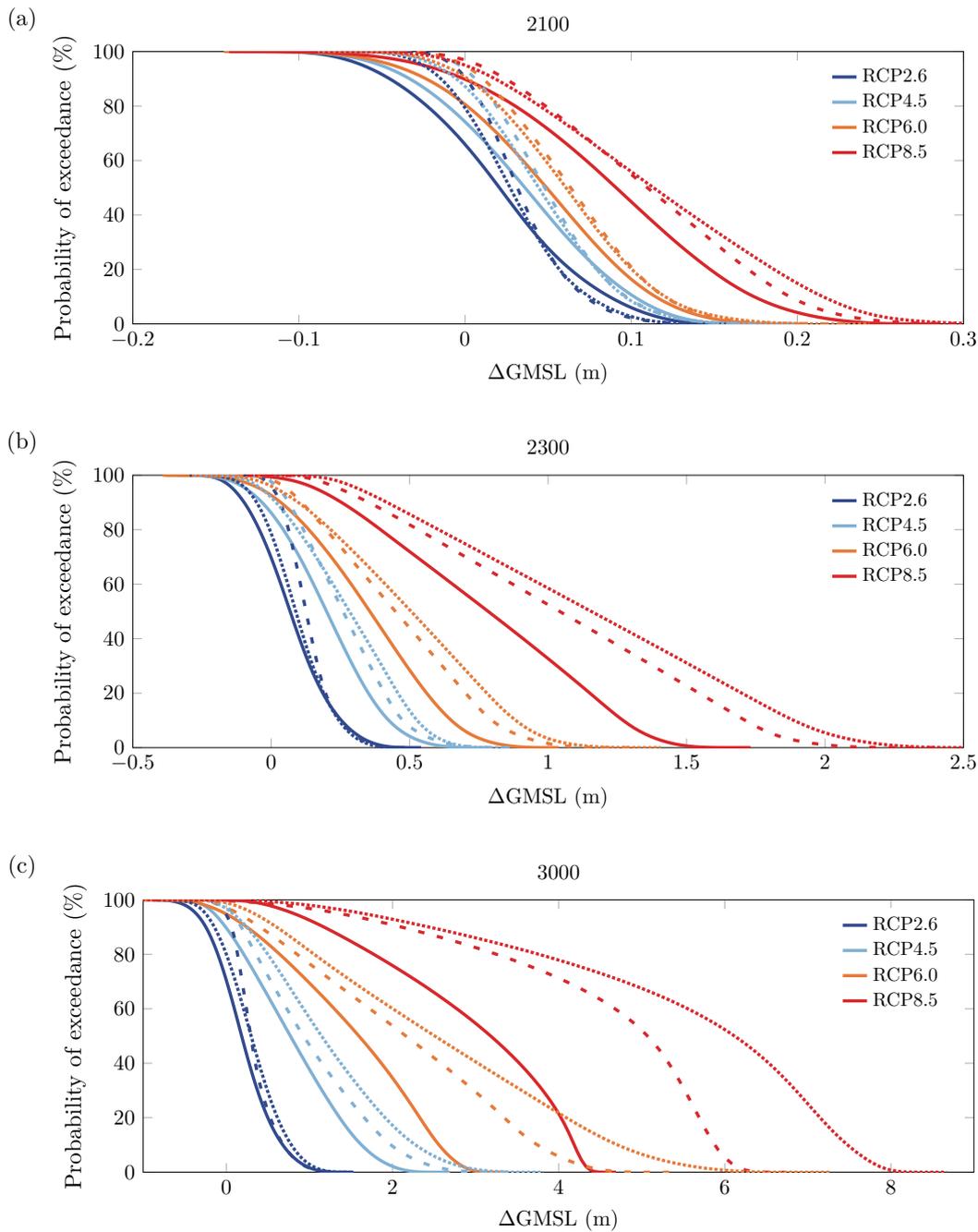
Figure 6. Probability of exceeding threshold values for sea-level rise evaluated as the complementary cumulative distribution functions of the probability density functions for sea-level rise projections. Probability of exceedance at 2100, (**b**) at 2300 and (**c**) at 3000 under the viscous sliding law (solid lines), the weakly nonlinear sliding law (dashed lines) and the strongly nonlinear sliding law (dotted lines).
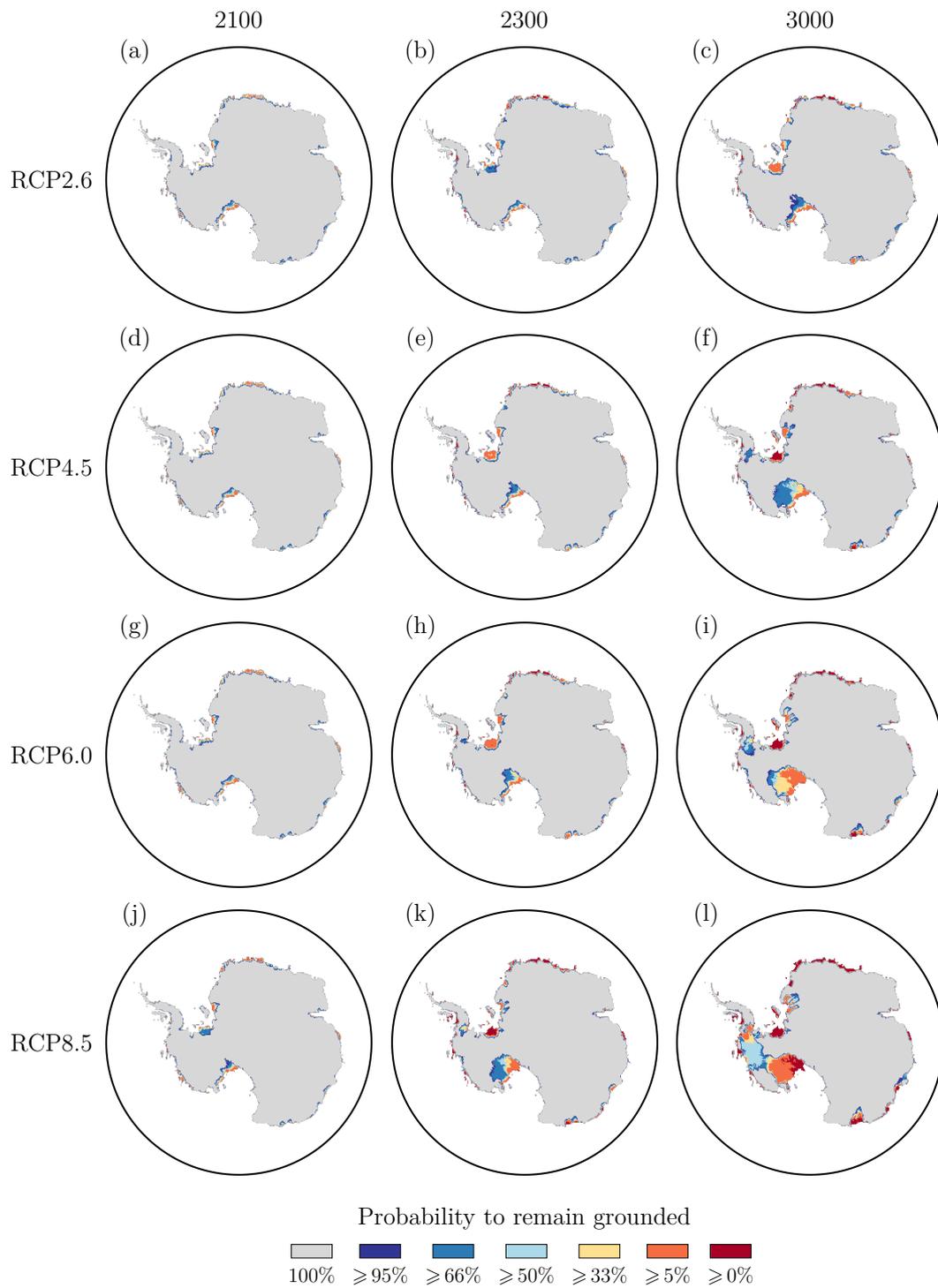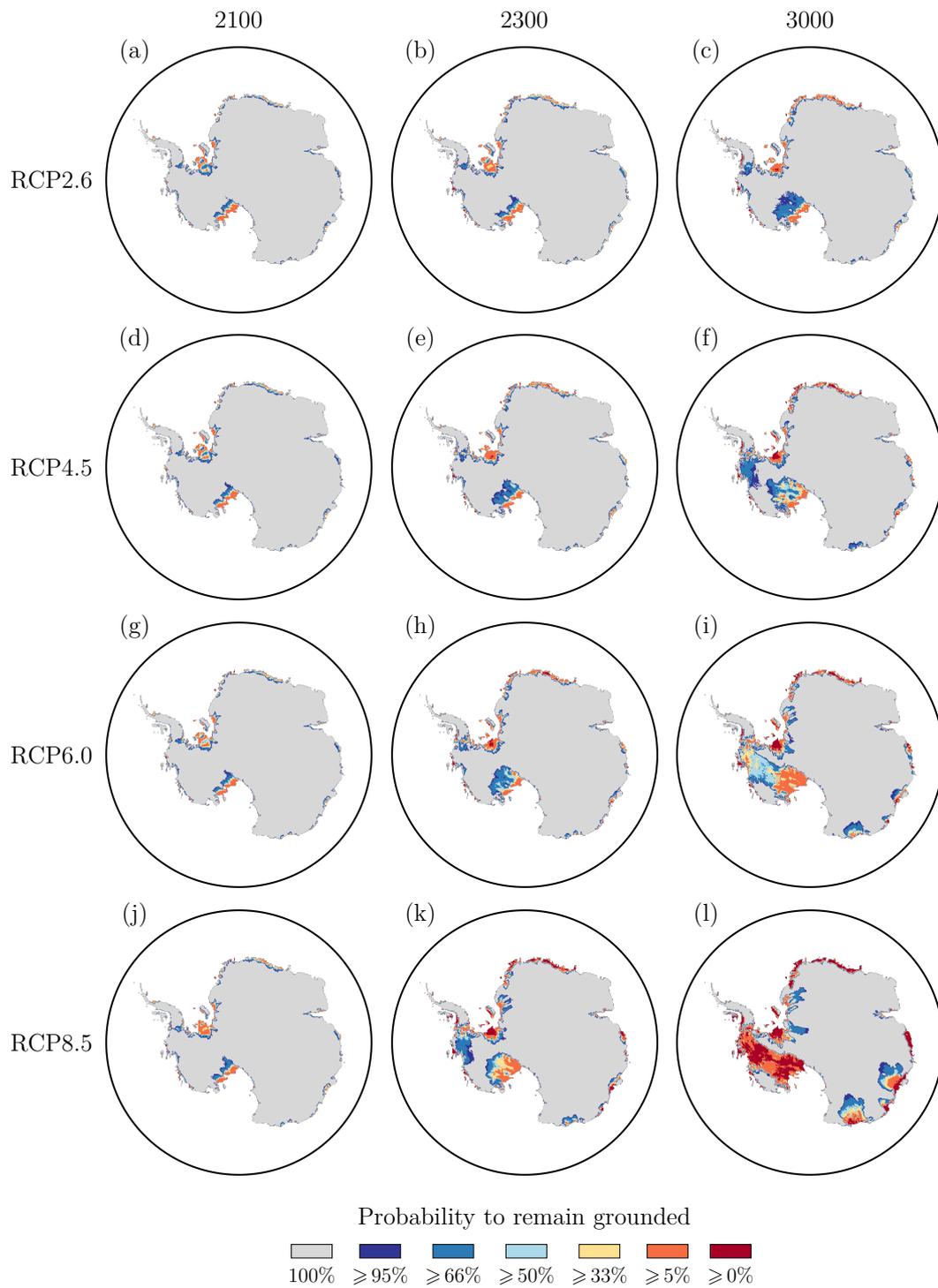
Figure 7. Confidence regions for grounded ice under sliding law with exponent $m = 1$. Confidence regions are shown at (**a**, **d**, **g**, **j**) 2100, (**b**, **e**, **h**, **k**) 2300 and (**c**, **f**, **i**, **l**) 3000.
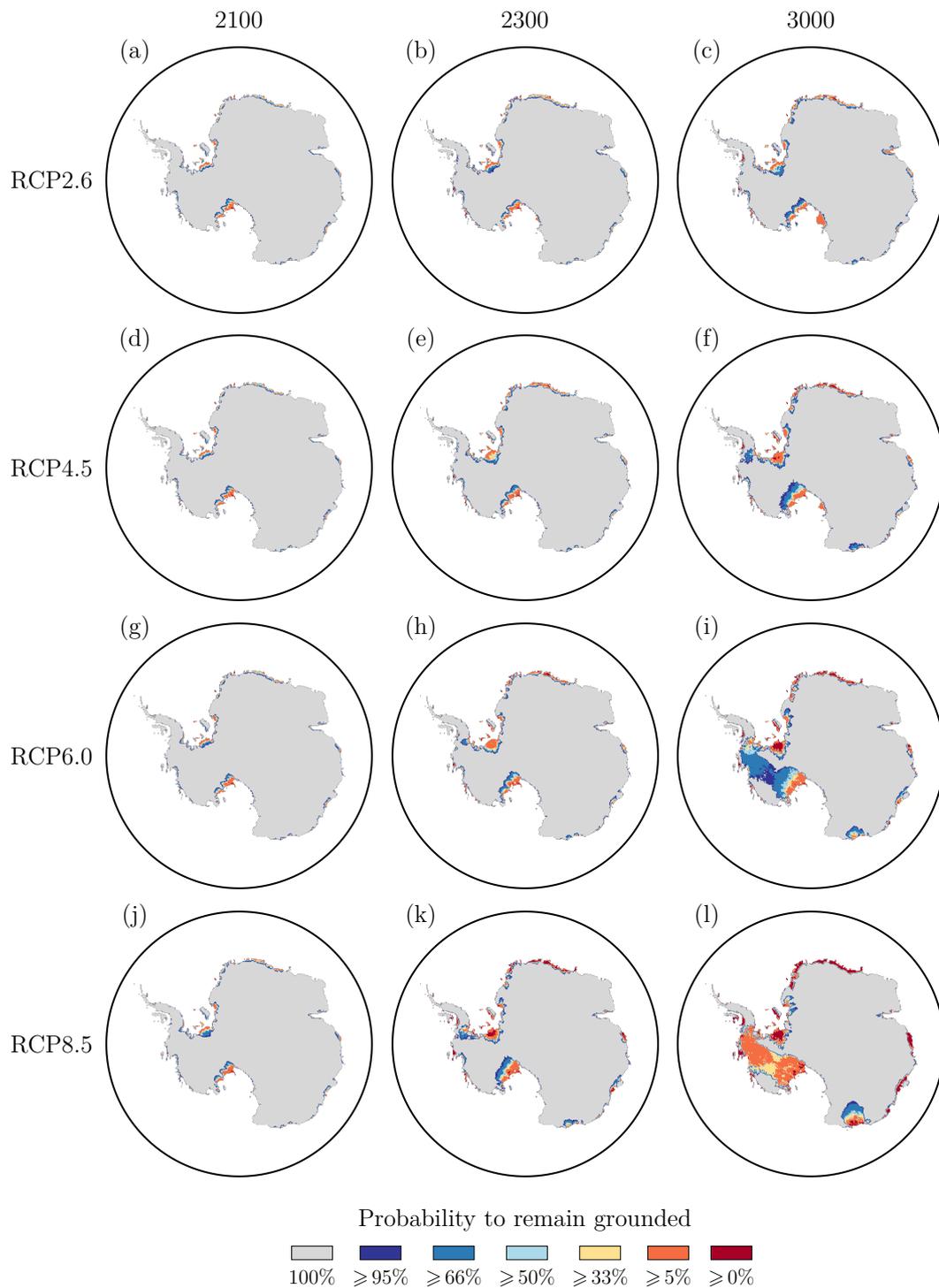
Figure 8. Confidence regions for grounded ice under sliding law with exponent $m = 3$. Confidence regions are shown at (**a**, **d**, **g**, **j**) 2100, (**b**, **e**, **h**, **k**) 2300 and (**c**, **f**, **i**, **l**) 3000.
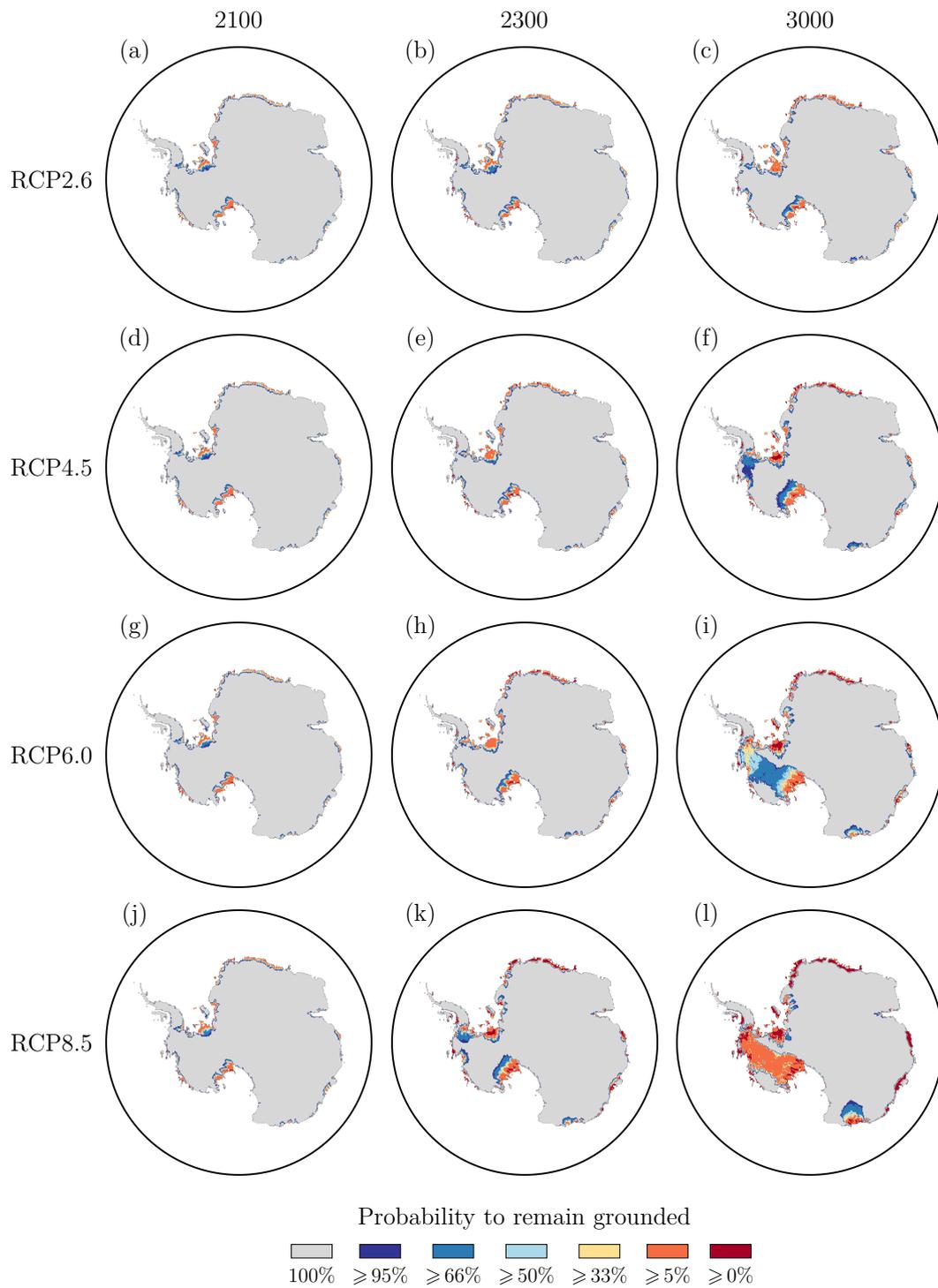
Figure 9. Confidence regions for grounded ice under sliding law with exponent $m = 5$. Confidence regions are shown at (**a**, **d**, **g**, **j**) 2100, (**b**, **e**, **h**, **k**) 2300 and (**c**, **f**, **i**, **l**) 3000.

Figure 10. Confidence regions for grounded ice under sliding law with exponent $m = 5$ and Tsai's grounding-line parameterisation. Confidence regions are shown at (**a**, **d**, **g**, **j**) 2100, (**b**, **e**, **h**, **k**) 2300 and (**c**, **f**, **i**, **l**) 3000.